Hindawi
Shock and Vibration
Volume 2019, Article ID 8376781, 16 pages
https://doi.org/10.1155/2019/8376781

Research Article

Optimisation Design and Damping Effect Analysis of Large Mass Ratio Tuned Mass Dampers

Ying-jie Kang and Ling-yun Peng

Beijing Key Laboratory of Earthquake Engineering and Structural Retrofit, Beijing University of Technology, Beijing 100124, China

Correspondence should be addressed to Ling-yun Peng; ply@bjut.edu.cn

Received 1 August 2018; Revised 10 December 2018; Accepted 3 January 2019; Published 27 January 2019

Academic Editor: Vadim V. Silberschmidt

Under harmonic load and random stationary white noise load, the existing fitting formulas are not suitable for calculating the optimal parameters of large mass ratio tuned mass dampers (TMDs). For this reason, the optimal parameters of large mass ratio TMDs are determined by numerical optimisation methods, and a revised fitting formula is proposed herein based on a curve fitting technique. Finally, the dynamic time history analysis method is used to study the control effect of large mass ratio TMDs. The results show that when the mass ratio is large, the error between the existing fitting formula and the actual optimal value is quite large, and the revised fitting formula is applicable to the parameter design of the traditional small mass ratio and large mass ratio (≤1) TMDs. When the ratio of local base soil predominant frequency to structure vibration frequency is greater than 4, the optimal parameters of a TMD under white noise excitation can be calculated according to the revised fitting formula, and the remaining conditions should be determined by numerical optimisation. In addition, a large mass ratio TMD reduces the dynamic response of the main structure effectively compared with a small mass ratio TMD and reduces the relative displacement between the TMD and main structure.

1. Introduction

In the field of civil engineering, the tuned mass damper (TMD) has been widely studied and applied as a vibration control technology [1, 2]. The scope of the technology's use involves, e.g., super high-rise structures [3], towering structures [4, 5], and long span structures [6]. With regard to the development of TMD optimisation design theory, the TMD optimal parameters (optimal frequency ratio and optimal damping ratio) of a single degree of freedom (SDOF) structure without damping under harmonic load were given by Den Hartog as early as 1956 [7]. Subsequently, with different dynamic responses as optimisation objectives, the formula for calculating TMD optimal parameters under different load excitation conditions was supplemented and expanded [8]. When considering the damping ratio of the main structure, the optimal parameters of a TMD often need to be obtained by a numerical optimisation method, and the formula itself is obtained by a curve fitting technique [9, 10]. Under the excitation of harmonic load or white noise random load, the fitting formula for calculating the optimal frequency ratio and the optimal damping ratio of a TMD contains only two variables: (1) the mass ratio between the TMD and the main structure and (2) the damping ratio of the main structure [11–13]. The existing research results show that the greater the mass ratio of TMD, the better the control effect on the structure. In a traditional TMD vibration damping structure, the construction of the TMD often requires additional mass blocks. For large structures and super high-rise structures, the mass ratio can only reach 2–5%, considering the influence of installation and cost. Therefore, the existing fitting formula often considers only the traditional mass ratio of less than 0.1, which is seldom involved in the calculation of the optimal parameters of a large mass ratio TMD.

From the control idea of tune frequency to reduction vibration, on the premise of ensuring that the local structure can satisfy its normal use function, the local structure is selected as the mass block of the TMD. Then, the nontraditional large mass ratio (>0.15) TMD is formed, such as the structure local isolation [6], the mega-substructure configuration [14, 15], and the interlayer isolation structure system [16, 17]. The noncritical components in the structure, such as filled walls and floors, can also be used as the mass blocks to form a large mass ratio TMD [18, 19]. In addition, the heavy equipment in an industrial plant can be constructed into a large mass ratio TMD in the form of suspension or isolation [20]. For example, in the typical coal-fired power plant, non-structural coal buckets are used as the mass blocks of TMD or MTMD, which are called the coal bucket dampers. In the side-coal-bunker thermal power plant structure, the mass ratio of coal buckets to the structure is nearly 0.5 [21–23]. When the main mode is controlled in a multi degree of freedom structure, the modal mass ratio of some TMDs can even reach values greater than 1 [24]. Some scholars have studied the parameter optimisation design of large mass ratio TMDs and their damping control effect. The results show that compared with the traditional small mass ratio TMD, the large mass ratio TMDs are effective in improving the seismic performance of the structure and are significantly robust in relation to the change of system parameters [6, 16, 24].

Against the background of good vibration control effects of large mass ratio TMDs, it remains to be determined whether the existing optimal parameter fitting formula is suitable for calculating the optimal parameters of large mass ratio TMDs. Therefore, based on previous studies, the error analysis and revision of the fitting formula of TMD optimal parameters are carried out in this study. The paper is organised as follows: first, the optimisation objective function and the optimisation analysis method of an SDOF structure with a TMD under seismic excitation are determined. Then, the optimal parameter fitting formula of the TMD is revised for excitations in the form of harmonic and white noise loads. Hence, the formula is also suitable for the design of large mass ratio TMDs. Subsequently, a detailed numerical optimisation is performed for the excitation of filtered white noise loads. Finally, a time history analysis method is used to investigate the effectiveness of large mass ratio TMDs on controlling the dynamic response of structures under seismic loading.

2. Dynamic Equilibrium Equation and Statement of the Optimisation Problem

The schematic diagram of an SDOF structure equipped with a TMD is shown in Figure 1. As a substructure, the TMD is connected to the main structure through the spring and damper. The main structure is characterised by its mass m_1, stiffness k_1, and damping c_1. Similar to the main structure, the TMD also has the properties of mass m_2, stiffness k_2, and damping c_2.

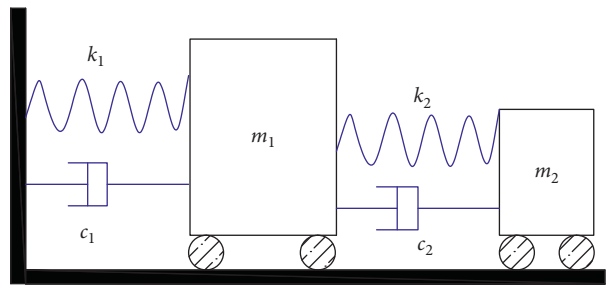

Figure 1: SDOF structure equipped with a TMD.

2.1. Dynamic Equilibrium Equation. The displacement, velocity, and acceleration of the main structure relative to the ground are defined as x_1, $\dot{x}_1$, and $\ddot{x}_1$, respectively. Similarly, the displacement, velocity, and acceleration of the TMD relative to the ground are defined as x_2, $\dot{x}_2$, and $\ddot{x}_2$, respectively. When the whole structure is subjected to base acceleration $\ddot{x}_g$, the dynamic equilibrium equation of the whole system is as follows:

$$\begin{cases} m_1\ddot{x}_1 + c_1\dot{x}_1 + k_1x_1 + c_2(\dot{x}_1 - \dot{x}_2) + k_2(x_1 - x_2) = -m_1\ddot{x}_g, \\ m_2\ddot{x}_2 + c_2(\dot{x}_2 - \dot{x}_1) + k_2(x_2 - x_1) = -m_2\ddot{x}_g. \end{cases} \tag{1}$$

Let $\ddot{x}_g = e^{i\omega t}$ and the displacement transfer function of the main structure be $h_1(\omega)$; then, $x_1 = h_1(\omega)e^{i\omega t}$. The expression for $h_1(\omega)$ can be obtained as

$$\begin{aligned} h_1(\omega) &= -\frac{m_1 + Z_1(\omega)}{(-\omega^2 m_1 + i\omega c_1 + k_1) - \omega^2 Z_1(\omega)}, \\ Z_1(\omega) &= \frac{m_2(i\omega c_2 + k_2)}{(-\omega^2 m_2 + i\omega c_2 + k_2)}, \end{aligned} \tag{2}$$

where $\omega_1 = \sqrt{k_1/m_1}$ and $\zeta_1 = c_1/2m_1\omega_1$ denote the natural frequency and viscous damping ratio of the main structure, respectively. The natural frequency and viscous damping ratio of the TMD are denoted as $\omega_2 = \sqrt{k_2/m_2}$ and $\zeta_2 = c_2/2m_2\omega_2$, respectively. The mass and tuning frequency ratio of the TMD are denoted as $\mu = m_2/m_1$ and $f = \omega_2/\omega_1$, respectively. The ratio of the excitation frequency to the natural frequency of the main structure is defined as $g = \omega/\omega_1$. Finally, the following expression can be obtained:

$$h_1(\omega) = \frac{1}{\omega_1^2} \cdot \frac{-(1+\mu)(2igf\zeta_2 + f^2 - g^2) - \mu g^2}{(-g^2 + 2ig\zeta_1 + 1 - g^2\mu)(-g^2 + 2igf\zeta_2 + f^2) - \mu g^4}. \tag{3}$$

(1) Under the excitation of harmonic load, the dynamic amplification factor $R_1 = |\omega_1^2 x_1/\ddot{x}_g|$ of the main structure is

$$R_1 = \sqrt{\frac{\left[(1+\mu)f^2 - g^2\right]^2 + 4g^2 f^2 \zeta_2^2 (1+\mu)^2}{\left[\mu g^2 f^2 + 4g^2 f \zeta_1 \zeta_2 - (g^2-1)(g^2-f^2)\right]^2 + 4g^2\left[\zeta_1 (g^2-f^2) + f\zeta_2 (g^2+\mu g^2-1)\right]^2}}. \tag{4}$$

(2) Under the excitation of random load, the mean square displacement response σ_1^2 of the main structure is given by

$$\sigma_1^2 = \int_{-\infty}^{+\infty} \left|h_1(\omega)\right|^2 S(\omega)\, d\omega, \tag{5}$$

where $S(\omega)$ denotes the spectral density function of random loads. If the external force is modelled as a Gaussian white noise with constant power spectral density, that is, $S(\omega) = S_0$, then σ_1^2 is given by

$$\sigma_1^2 = \frac{2\pi S_0}{\omega_1^3}\left[\frac{\zeta_2\left[1 + f^2(\mu-2)(1+\mu)^2 + f^4(1+\mu)^4 + 4f^2(1+\mu)^3\zeta_2^2\right] + 4f^2(1+\mu)^2\zeta_1^2\zeta_2 + \mu f\zeta_1\left(\mu + f^2(1+\mu)^2\right) + 4f\zeta_1\zeta_2^2(1+\mu)^2\left(1+f^2(1+\mu)\right)}{4\left[\zeta_1\zeta_2\left\{1 - 2f^2 + f^4(1+\mu)^2 + 4f^2\zeta_2^2(1+\mu)\right\} + \mu f\zeta_2^2 + \mu f^3\zeta_1^2 + 4f^2\zeta_1^3\zeta_2 + 4f\zeta_1^2\zeta_2^2\left(1+f^2(1+\mu)\right)\right]}\right]. \tag{6}$$

2.2. Optimisation Analysis. The displacement response of the main structure is taken as the evaluation index of the TMD damping effect. Under a certain mass ratio μ, the optimal objective function is as follows:

(1) Under the excitation of harmonic load,

$$\min R_1(f, \zeta_2). \tag{7}$$

(2) Under the excitation of random load,

$$\min \sigma_1^2(f, \zeta_2). \tag{8}$$

For a main structure with no damping, i.e., for $\zeta_1 = 0$, theoretical solutions of the TMD optimal design parameters can be obtained as suggested in [8]:

(1) Under the excitation of harmonic load,

$$f_{\text{opt}} = \frac{\sqrt{1-\mu/2}}{1+\mu}, \qquad \zeta_{2\text{opt}} = \sqrt{\frac{3\mu}{4(2-\mu)(1+\mu)}}. \tag{9}$$

(2) Under the excitation of random load,

$$f_{\text{opt}} = \frac{\sqrt{1-\mu/2}}{1+\mu}, \qquad \zeta_{2\text{opt}} = \sqrt{\frac{\mu(1-\mu/4)}{4(1+\mu)(1-\mu/2)}}, \tag{10}$$

where f_{opt} and ζ_{opt} denote the optimal frequency ratio and the optimal damping ratio of the TMD, respectively.

For a damped main structure, i.e., for $\zeta_1 \neq 0$, the theoretical derivation of the optimal design parameters of the TMD is very complicated. Therefore, numerical optimisation is often used to obtain the optimal parameters. The common numerical optimisation methods include the following:

(1) The discretisation of independent variables and derivation of their corresponding objective function values, followed by the selection of the optimal values and corresponding variables from them [11]. This method is called DO in short.

(2) Genetic algorithm optimisation methods. This method is called GA in short.

(3) Particle swarm optimisation methods. This method is called PSO in short [13].

The MATLAB software provides an optimisation toolbox (OT), which can also solve multiple nonlinear function optimisation problems. Under the excitation of random load, three methods including DO, PSO, and OT are used to solve the optimal parameters of TMD. The damping ratio of the main structure is set to 0, so as to compare with the theoretical solution. Figure 2 shows the calculation results of the TMD optimal parameters by DO, PSO, and OT. The results calculated by the theoretical equation (10) are also plotted. It can be seen that the optimal frequency ratio f_{opt} decreases logarithmically with the increase of mass ratio μ, while the optimal damping ratio ζ_{opt} increases logarithmically with the increase of mass ratio μ. In addition, it can also be seen that the optimal parameters obtained by the three optimisation methods are consistent with the theoretical results, indicating the accuracy of the numerical optimisation method. Based on the consideration of simplicity and

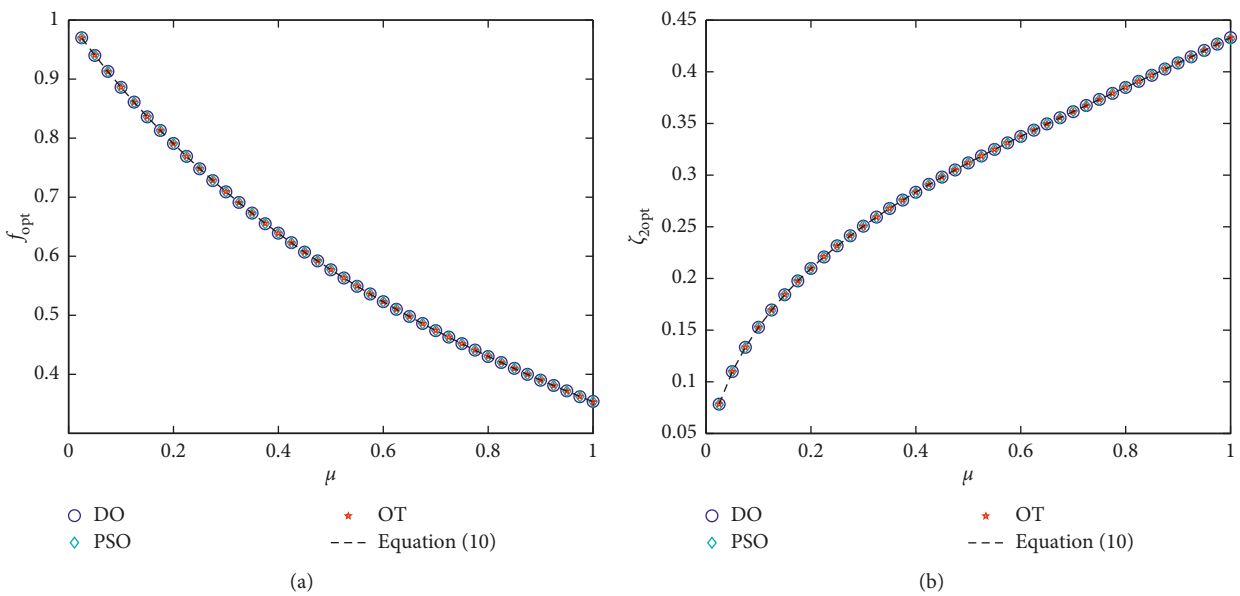

Figure 2: Comparison of numerical optimisation algorithms and theoretical results. (a) Optimisation results of the frequency ratio. (b) Optimisation results of the damping ratio.

efficiency, the MATLAB OT is used for numerical optimisation.

3. Fitting Formula for Optimal TMD Parameters under Harmonic Load and Error Analysis

Under harmonic excitation, the fitting formula for the TMD optimal frequency ratio and optimal damping ratio is given in reference [10], as shown below:

$$\begin{aligned} f_{\text{opt}} &= \left(\frac{\sqrt{1-\mu/2}}{1+\mu} + \sqrt{1-2\zeta_1^2} - 1\right) \\ &\quad - (2.375 - 1.034\sqrt{\mu} - 0.426\mu)\sqrt{\mu}\zeta_1 \\ &\quad - (3.730 - 16.903\sqrt{\mu} + 20.496\mu)\sqrt{\mu}\zeta_1^2, \end{aligned} \tag{11}$$

$$\begin{aligned} \zeta_{2\text{opt}} &= \sqrt{\frac{3\mu}{4(2-\mu)(1+\mu)}} + \left(0.151\zeta_1 - 0.170\zeta_1^2\right) \\ &\quad + \left(0.163\zeta_1 + 4.980\zeta_1^2\right)\mu. \end{aligned}$$

The above optimisation analysis method is used to obtain the optimal parameters of different mass ratio TMDs, as shown in Figure 3. The calculated values of the fitting formula corresponding to the main structure with different damping ratios are also plotted. It can be seen that when the mass ratio is less than 0.2, the optimal parameters obtained from the fitting formula are in good agreement with the actual optimal parameters, which can meet practical design requirements. With the increase of the mass ratio, the fitting formula value of the optimal parameters deviates from the actual optimal value, and the error increases. The fitting formula value of the optimal frequency ratio is smaller than the actual value, and the error increases with the increase of main structure damping. When the damping ratio ζ_1 is 0.1 and the mass ratio μ is greater than 0.55, the error is greater than 5.5%. At the same time, when the damping ratio ζ_1 is 0.02, the error of the fitting formula value for the optimal damping ratio is the smallest. When the damping ratio ζ_1 is 0.1 and the mass ratio μ is greater than 0.75, the error is greater than 5.35%. On the whole, when the mass ratio μ is large, the error of the existing fitting formula is very obvious.

Based on the above analysis, the fitting formula in equation (11) is not suitable for calculating the optimal parameters of large mass ratio TMDs. Therefore, a curve fitting method is used to revise the formula, and the new fitting formula is obtained as follows:

$$\begin{aligned} f_{\text{opt}} &= \left(\frac{\sqrt{1-\mu/2}}{1+\mu} + \sqrt{1-2\zeta_1^2} - 1\right) \\ &\quad + (-2.6976 + 2.5809\sqrt{\mu} - 0.9656\mu)\sqrt{\mu}\zeta_1 \\ &\quad + (-1.5547 + 5.3501\sqrt{\mu} - 4.3634\mu)\sqrt{\mu}\zeta_1^2, \\ \zeta_{2\text{opt}} &= \sqrt{\frac{3\mu}{4(2-\mu)(1+\mu)}} + (0.9614 - 0.5667\sqrt{\mu} - 0.1277\mu) \\ &\quad \cdot \sqrt{\mu}\zeta_1 + (20.5477 - 67.8430\sqrt{\mu} + 62.6722\mu)\mu\zeta_1^2. \end{aligned} \tag{12}$$

Figure 4 shows the relationship between the calculated value of the revised fitting formula and the actual optimal value, and the change curve of the error rate along with the mass ratio is shown in Figure 5. The calculation method of the error rate is as follows:

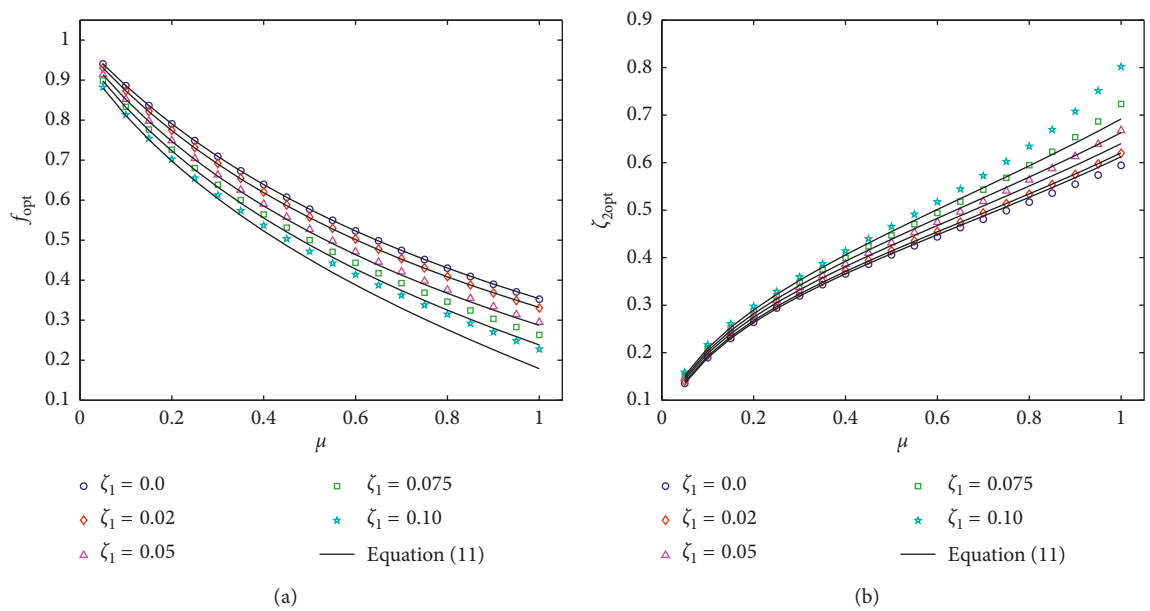

Figure 3: The curve of the calculated value of the existing fitting formula and the actual optimal value varies with the mass ratio under the excitation of harmonic load. (a) Contrast results of the frequency ratio. (b) Contrast results of the damping ratio.

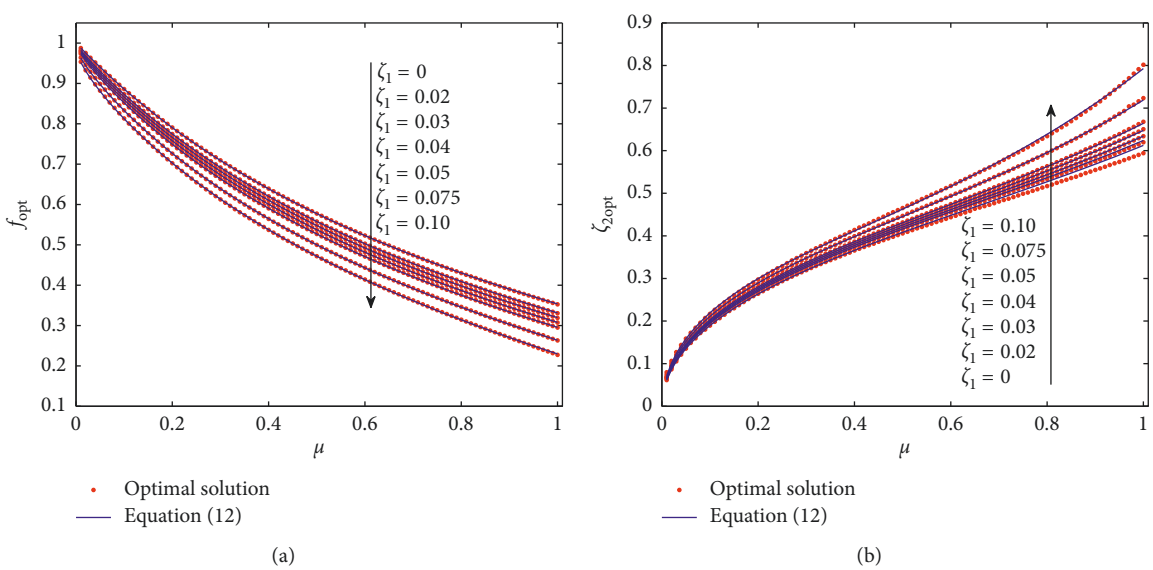

Figure 4: The relationship between the revised fitting formula value and the actual optimal value with the TMD mass ratio and the damping ratio of the main structure under the excitation of harmonic load. (a) Optimal frequency ratio. (b) Optimal damping ratio.

$$\text{Error} = \frac{\left(f_{\text{opt\_Form}} - f_{\text{opt\_Num}}\right)}{f_{\text{opt\_Num}}} \times 100,$$
$$\text{Error} = \frac{\left(\zeta_{2\text{opt\_Form}} - \zeta_{2\text{opt\_Num}}\right)}{\zeta_{2\text{opt\_Num}}} \times 100, \tag{13}$$

where $f_{\text{opt\_Form}}$ and $\zeta_{\text{opt\_Form}}$ are the TMD optimal values calculated using the revised fitting formula in equation (12). The actual optimal values obtained by a numerical optimisation method are $f_{\text{opt\_Num}}$ and $\zeta_{2\text{opt\_Num}}$.

It can be seen that the error between the optimal frequency ratio calculated by the revised fitting formula and the actual optimal value is smaller. When the damping ratio of the main structure is 0~0.1, the maximum error rate is less than 1%. When the mass ratio is less than 0.02, the error is relatively large. This is mainly due to the relatively small TMD damping ratio, which leads to a relatively large error rate. Under the condition of different mass ratio TMDs, the error rate can be kept within 5%.

On the whole, the error of the revised fitting formula is small, which can meet actual design requirements of a large mass ratio TMD under harmonic excitation.

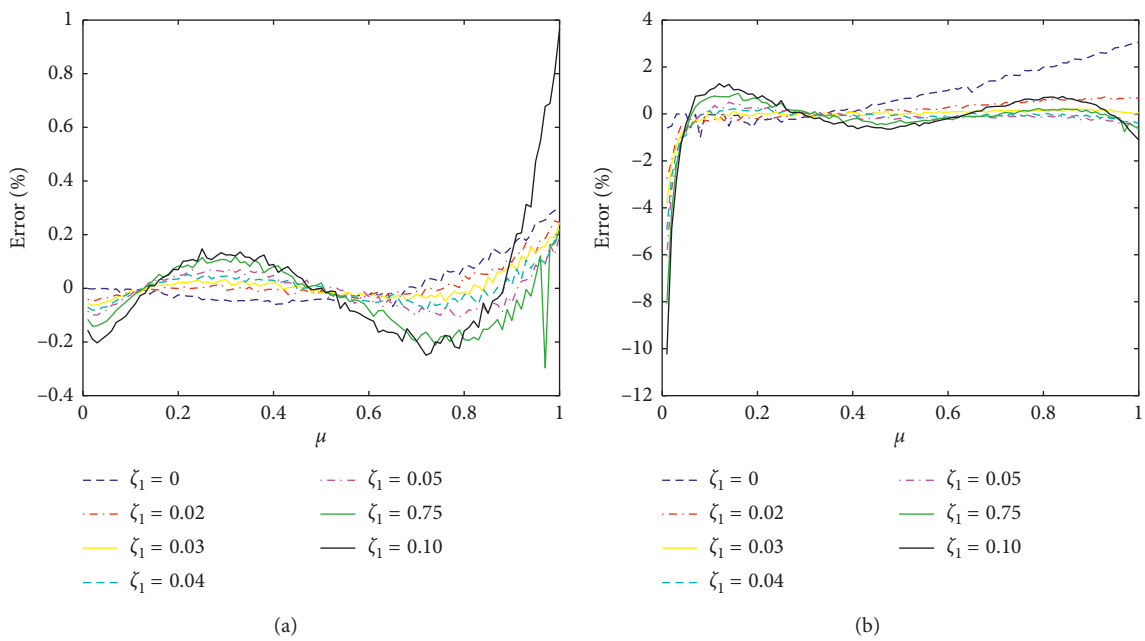

Figure 5: The error rate of the revised fitting formula value with the TMD mass ratio and the damping ratio of the main structure under the excitation of harmonic load. (a) Error rate of the frequency ratio. (b) Error rate of the damping ratio.

4. Fitting Formula for Optimal TMD Parameters under Random Load and Error Analysis

4.1. Stationary White Noise Random Load. Under stationary white noise excitations, the fitting formula of the TMD optimal frequency ratio and optimal damping ratio is given in reference [11], as shown below:

$$f_{\text{opt}} = \frac{\sqrt{1-\mu/2}}{1+\mu} + (-3.79441 + 9.87259\sqrt{\mu} - 15.2978\mu) \cdot \sqrt{\mu}\zeta_1 + (-13.6731 + 19.1284\sqrt{\mu} + 21.7049\mu)\sqrt{\mu}\zeta_1^2,$$
$$\zeta_{2\text{opt}} = \sqrt{\frac{\mu(1-\mu/4)}{4(1+\mu)(1-\mu/2)}}. \tag{14}$$

However, the fitting formula only considers the case that the mass ratio is less than 0.1. When the mass ratio of TMD is greater than 0.1, the relationship between the optimal value calculated by the fitting formula in equation (14) and the actual optimal value is shown in Figure 6. In equation (14), the optimal value of the damping ratio is independent of ζ_1; consequently, there is only a curve for all considered values of ζ_1 in Figure 6(b). It can be seen that when the mass ratio is smaller than 0.2, the error between the optimal parameters calculated by the fitting formula and the actual optimal parameters is still relatively small. However, with the increase of the mass ratio, the error increases significantly. In addition, the error of the fitting formula increases with the increase of the damping ratio of the main structure. From the error results, the fitting formula in equation (14) is also not suitable for calculating the optimal parameters of large mass ratio TMDs. The new formula obtained by the curve fitting method is as follows:

$$f_{\text{opt}} = \frac{\sqrt{1-\mu/2}}{1+\mu} + (-2.9089 + 2.3354\sqrt{\mu} - 0.5790\mu)\sqrt{\mu}\zeta_1 + (-13.1740 + 30.7222\sqrt{\mu} - 21.2318\mu)\sqrt{\mu}\zeta_1^2,$$
$$\zeta_{2\text{opt}} = \sqrt{\frac{\mu(1-\mu/4)}{4(1+\mu)(1-\mu/2)}} + (-0.5747 + 1.5424\sqrt{\mu} - 0.7846\mu)\sqrt{\mu}\zeta_1 + (31.4166 - 96.8253\sqrt{\mu} + 73.9404\mu)\mu\zeta_1^2. \tag{15}$$

Under stationary white noise excitations, the relationship between the calculated value of the revised fitting formula and the actual optimal value is shown in Figure 7. The curve of error rate change relative to the mass ratio is shown in Figure 8. The calculation method of the error rate is the same as in equation (13).

The error between the optimal frequency ratio calculated by the revised fitting formula and the actual optimal value is small. The damping ratio of the main structure has an effect on the error. However, when the damping ratio is 0.1, the maximum error rate of the optimal frequency ratio is still below 1.2%. In addition, the error rate of the optimal damping ratio varies with the TMD mass ratio, but it can always be kept within 5%.

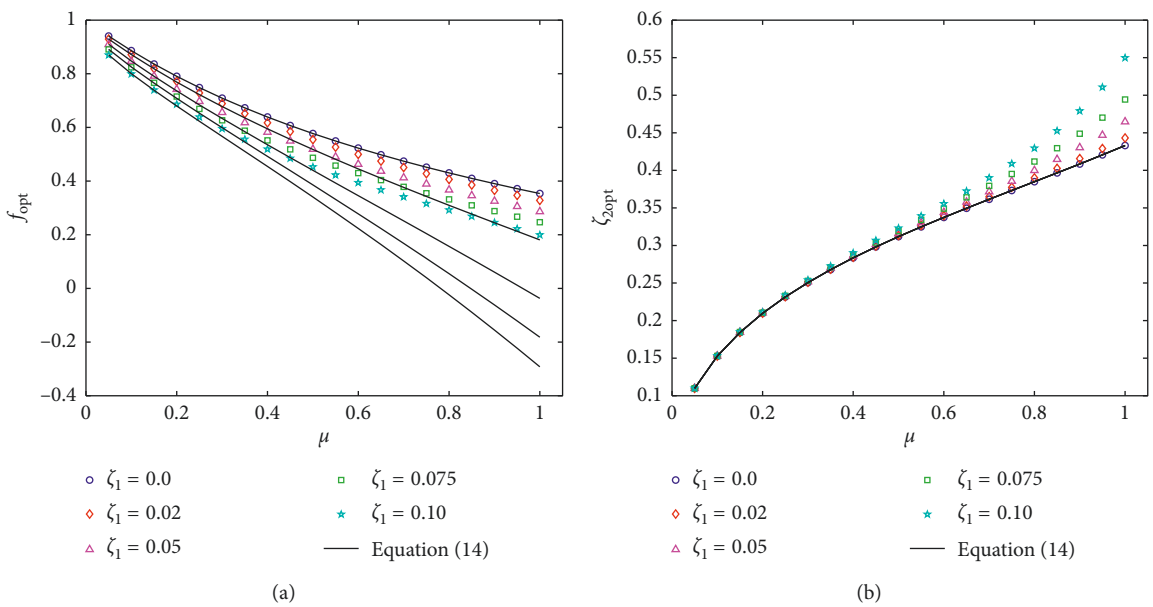

Figure 6: The curve of the calculated value of the existing fitting formula and the actual optimal value varies with the mass ratio under stationary white noise excitations. (a) Contrast results of the frequency ratio. (b) Contrast results of the damping ratio.

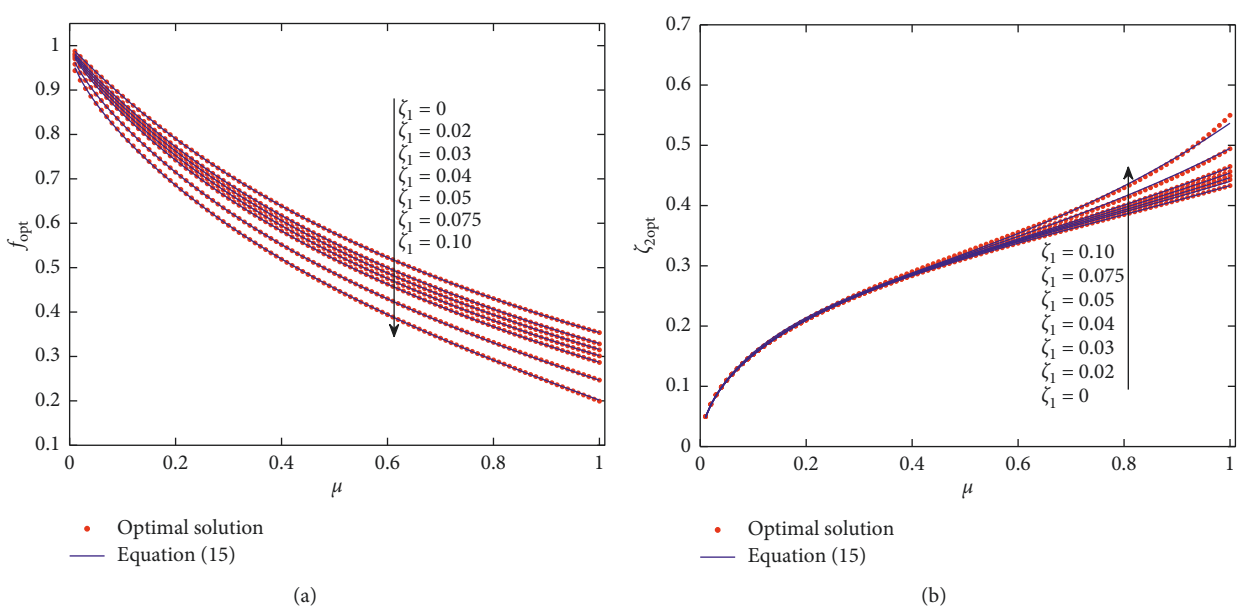

Figure 7: The relationship between the revised fitting formula value and the actual optimal value with the TMD mass ratio and the damping ratio of the main structure under stationary white noise excitations. (a) Optimal frequency ratio. (b) Optimal damping ratio.

On the whole, the error of the revised fitting formula is small, which meets actual design requirements of large mass ratio TMDs. Comparisons between the design method in reference [16] and that in this paper are illustrated in Table 1. It can be seen that the optimisation parameters in this study are obviously larger than those in reference [16]. This is mainly due to the inconsistency of the optimisation objectives of the two methods.

4.2. Filtered White Noise Random Load. The filtered white noise random load is modelled as proposed by Kanai [25]:

$$S(\omega) = \frac{\omega_g^4 + 4\zeta_g^2\omega_g^2\omega^2}{\left(\omega_g^2 - \omega^2\right)^2 + 4\zeta_g^2\omega_g^2\omega^2} S_0, \tag{16}$$

where ω_g and ζ_g are the predominant frequency and damping ratio of foundation soil, respectively.

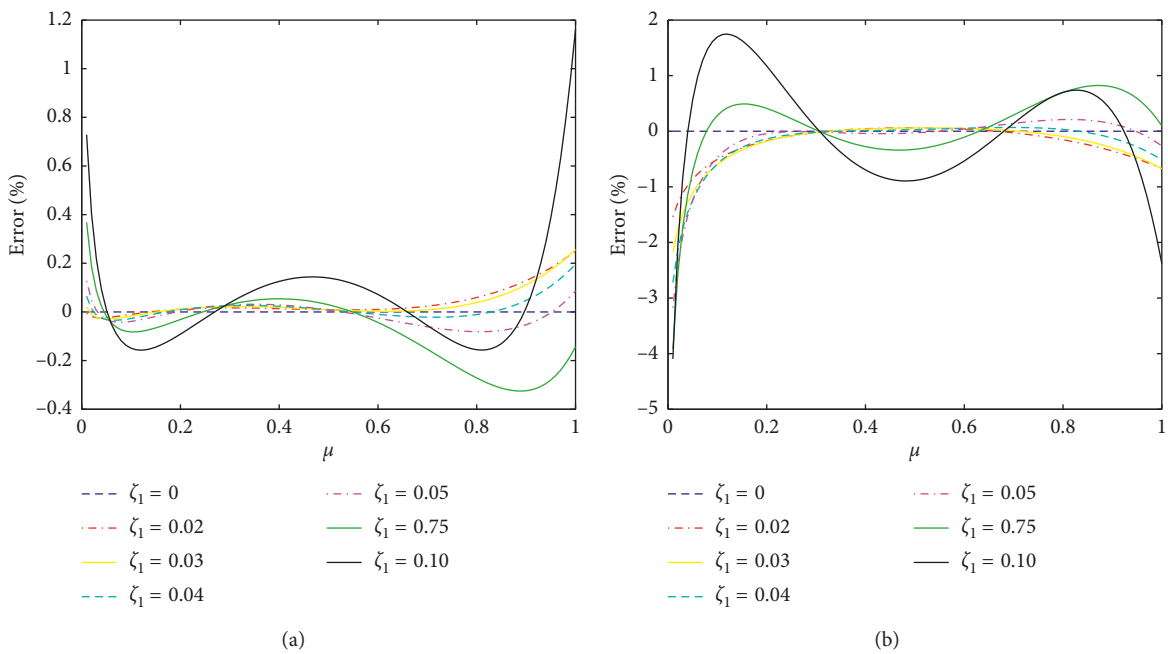

Figure 8: The error rate of the revised fitting formula value with the TMD mass ratio and the damping ratio of the main structure under stationary white noise excitations. (a) Error rate of the frequency ratio. (b) Error rate of the damping ratio.

Table 1: Optimal design of large mass ratio TMD according to reference [16] and this study.

Structural parameters	Method	f_{opt}	ζ_{opt}	$\sigma_1^2\,(2\pi S_0/\omega_1^3)$
$\mu = 0.431, \zeta_1 = 0.02$	Reference [16]	0.6871	0.2729	2.3830
	This study	0.5970	0.2939	2.2429
$\mu = 0.5, \zeta_1 = 0.02$	Reference [16]	0.6543	0.2900	2.3862
	This study	0.5549	0.3135	2.2246
$\mu = 0.5, \zeta_1 = 0.03$	Reference [16]	0.6492	0.2861	2.2947
	This study	0.5432	0.3144	2.1320

Substituting $S(\omega)$ into equation (5), the mean square of the structural displacement response is obtained as

$$\sigma_1^2 = \int_{-\infty}^{+\infty} \left|h_1(\omega)\right|^2 \frac{\omega_g^4 + 4\zeta_g^2\omega_g^2\omega^2}{\left(\omega_g^2 - \omega^2\right)^2 + 4\zeta_g^2\omega_g^2\omega^2} S_0\, d\omega. \tag{17}$$

Because solving equation (17) analytically is very tedious, a numerical integration method can be used. The results by Bakre [11] show that the TMD optimal parameters are relatively close when the structure is excited by white noise random load and filtered white noise random load, but only when a mass ratio below 0.1 is examined. The analysis result obtained by Hoang et al. [6] shows that there is a certain difference between the optimal parameters for the larger mass ratio TMD.

When solving the optimal parameters, the effect of the main structure damping ratio should be taken into account; the predominant frequency and damping ratio of the ground soil, that is, ω_g and ζ_g, are also taken into consideration. However, it is not practical to construct a corresponding fitting formula. Therefore, the optimisation process of TMD optimal parameters is described in detail, and the corresponding fitting formula is no longer determined. The detailed optimisation flow chart is shown in Figure 9. Firstly,

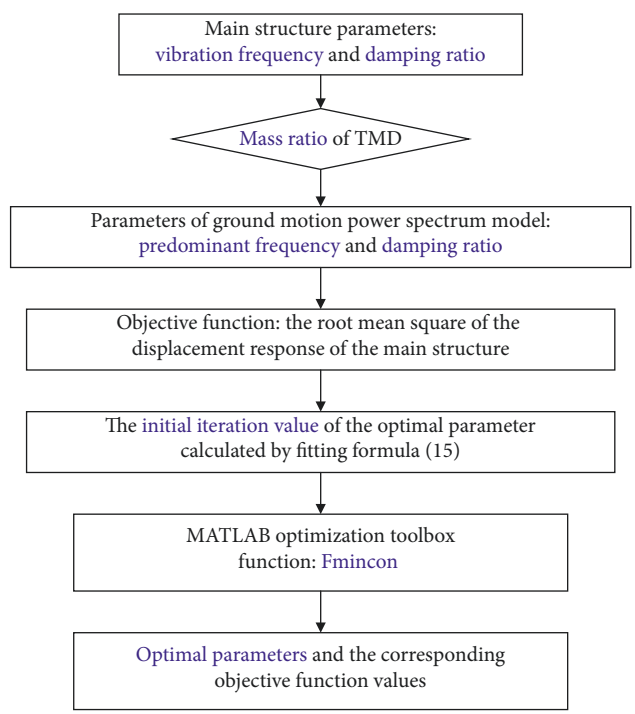

Figure 9: The numerical optimisation process of TMD parameters under filtered white noise excitations.

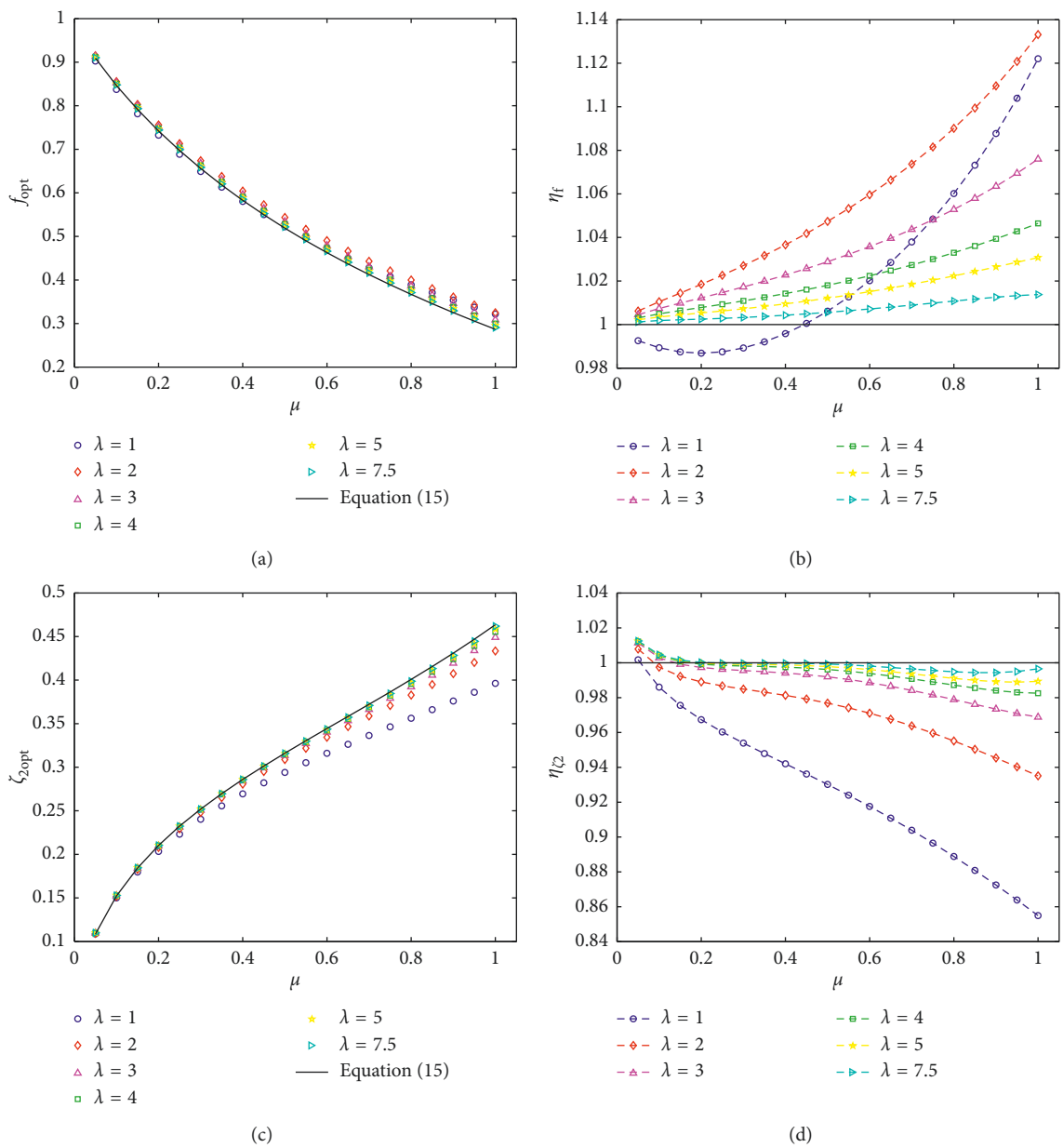

Figure 10: The relation between optimal parameters with λ and μ and its deviation rate with equation (15) under filtered white noise excitations. (a) Optimal frequency ratio. (b) η_f. (c) Optimal damping ratio. (d) $\eta_{\zeta_{2opt}}$.

the dynamic characteristics of the main structure, including natural frequency and damping ratio, are determined. Then, the mass ratio of TMD and site condition parameters, including the predominant frequency and damping ratio, are selected. After that, the objective of optimisation is determined, that is, the mean square of the structural displacement. Finally, taking the calculated value of equation (15) as the initial value, the optimal parameters can be obtained by optimum analysis using MATLAB optimisation toolbox.

Taking class II sites [26] as an example, the parameters of the Kanai-Tajimi model, $\omega_g = 15.708$, and $\zeta_g = 0.72$ are determined. S_0 is always taken as a constant, and it has no effect on TMD parameter optimisation. At the same time, $\lambda = \omega_g/\omega_1$ is defined as the ratio between the predominant frequency of filtered white noise and the natural frequency of the structure. In order to study the TMD optimal parameters and the relative relationship between the excitation of stationary white noise random load and filtered white noise random load, the following definitions are given:

$$\eta_f = \frac{f_{\text{opt\_Num}}}{f_{\text{opt\_Form}}},$$
$$\eta_{\zeta_2} = \frac{\zeta_{2\text{opt\_Num}}}{\zeta_{2\text{opt\_Form}}}. \tag{18}$$

Table 2: Seismic wave information used in the analyses.

Type	Name	Earthquake	Station	Component	Year
Far field	El Centro	Imperial valley	El Centro	N-S	1940
	Hachinohe	Tokachi-Oki	Hachinohe city	N-S	1968
Near field	Northridge	Northridge	SCH	N-S	1994
	Kobe	Hyogo-ken	KJMA	N-S	1995

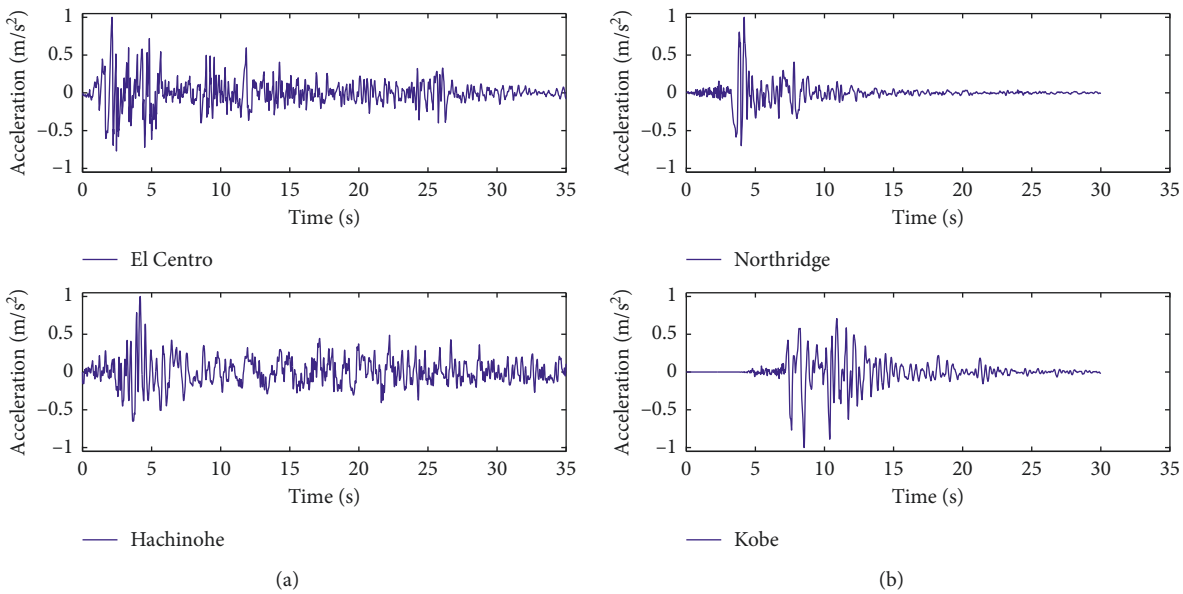

Figure 11: Time history curve of seismic records. (a) Far-field seismic waves. (b) Near-field seismic waves.

Under stationary white noise excitations, $f_{\text{opt\_Form}}$ and $\zeta_{\text{opt\_Form}}$ are the TMD optimal frequency ratios and the optimal damping ratios calculated by the fitting equation (15), respectively. Under filtered white noise excitations, $f_{\text{opt\_Num}}$ and $\zeta_{\text{opt\_Num}}$ are the TMD optimal frequency ratio and the optimal damping ratio, respectively, obtained by the numerical optimisation method.

When the main structure with a damping ratio of 0.05 is excited by filtered white noise load, the relationship between the optimal parameters of the TMD and μ and λ is shown in Figures 10(a) and 10(c). In order to facilitate comparison, the optimal parameter calculated by the fitting formula in equation (15) is also plotted. Figures 10(b) and 10(d) show, respectively, the trends of η_f and $\eta_{\zeta_{2\text{opt}}}$ with μ and for different values of λ.

From the above results, the following results are obtained.

When the mass ratio μ is smaller than 0.2, the optimal parameters of the stationary white noise random load and that of the filtered white noise random load are more similar, but the difference between the two is increased gradually with the increase of the mass ratio, which can be clearly seen from the relationship curve of η_f to μ.

The larger the λ, the more η_f and $\eta_{\zeta_{2\text{opt}}}$ become closer to 1. When $\lambda \geq 4$, even if the TMD mass ratio reaches 1, the error of the optimal parameters of the TMD under the stationary white noise random load and the filtered white noise random load is not more than 5%.

In addition, the damping ratio of the main structure has a relatively small impact on the error; therefore, the influence of the damping ratio of the main structure on the error of the fitting formula is no longer discussed in this paper. In conclusion, for the optimal design of a large mass ratio TMD, when $\lambda \geq 4$, the fitting formula in equation (15) is also suitable for filtered white noise excitations, while in the other cases, it is suggested to determine the optimal TMD parameters using a numerical optimisation method.

5. Damping Effect Analysis of a Large Mass Ratio TMD

Four SDOF structures with 0.5, 1.0, 2.0, and 3.0 s periods (T) are selected, and the damping ratio of the four structures is 0.05. The TMD mass ratios are 0.05, 0.25, 0.50, 0.75, and 1, and the TMD parameters are calculated by the fitting formula in equation (15). Two far-field seismic waves (El Centro, Hachinohe) and two near-field seismic waves (Northridge, Kobe) are used for load input [27]. Seismic wave information is provided in Table 2. The seismic wave acceleration-time history curve is shown in Figure 11, and

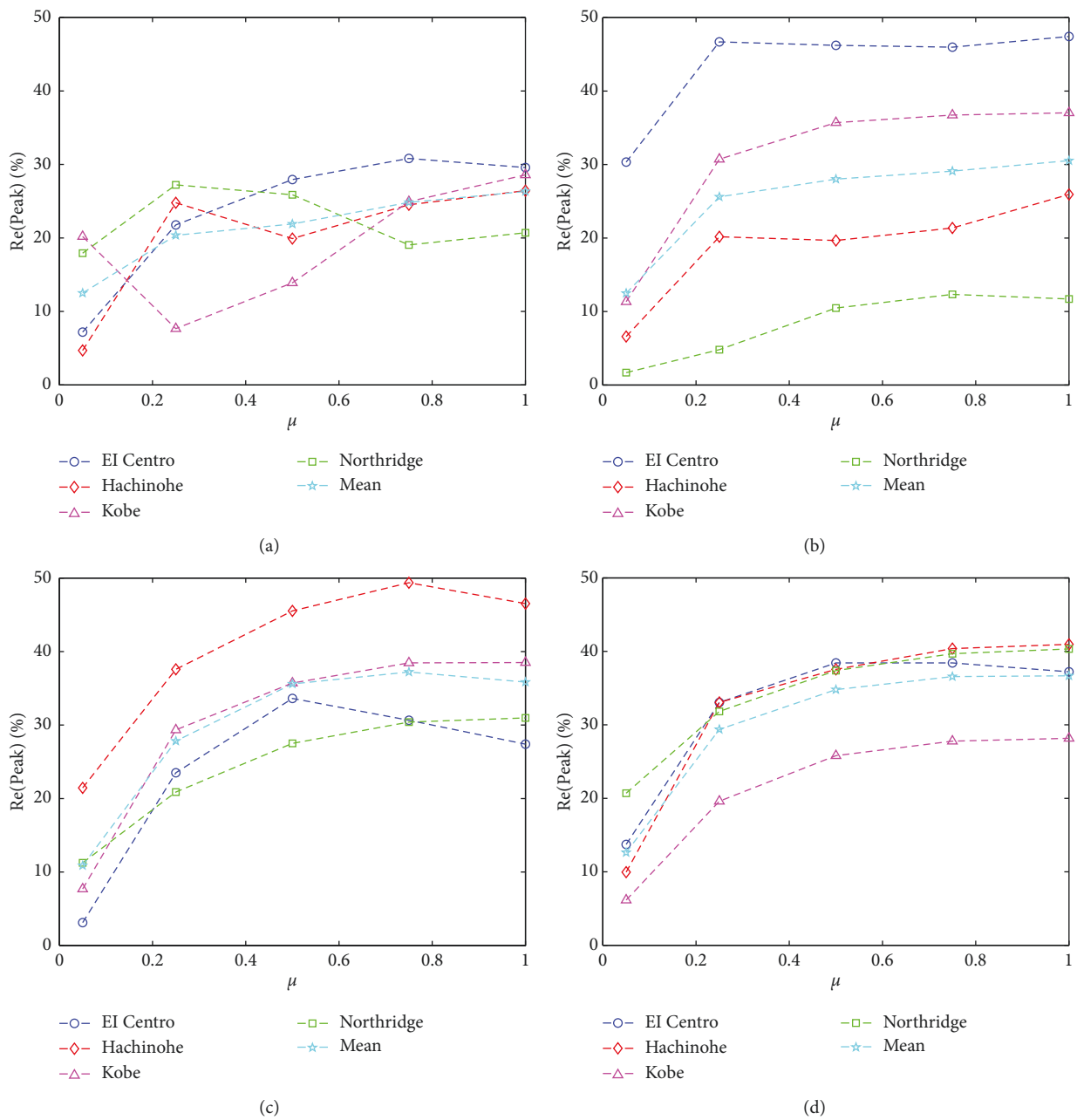

Figure 12: The damping effect of different mass ratio (TMD) on the peak value of structural displacement response. (a) $T = 0.5$ s. (b) $T = 1.0$ s. (c) $T = 2.0$ s. (d) $T = 3.0$ s.

the seismic wave peak value is 1 m/s^2. In order to investigate the effect of the TMD mass ratio on the control of the structural displacement response, four sets of seismic time history analyses were carried out for structures with and without a TMD, respectively.

The reduction rate of peak displacement Re(Peak) and the reduction rate of root mean square of structural displacement Re(RMS) are used as the evaluation index, respectively. The two formulas for calculating the damping rate are shown as follows:

$$\begin{aligned} \mathrm{Re}(\mathrm{Peak}) &= 1 - \frac{\mathrm{Max}(x_{\mathrm{TMD}})}{\mathrm{Max}(x)}, \\ \mathrm{Re}(\mathrm{RMS}) &= 1 - \frac{\mathrm{RMS}(x_{\mathrm{TMD}})}{\mathrm{RMS}(x)}, \end{aligned} \tag{19}$$

where x and x_{TMD} are the time history record of the displacement response of the structure without and with a TMD, respectively. The formula for calculating the root mean square of the displacement is as follows:

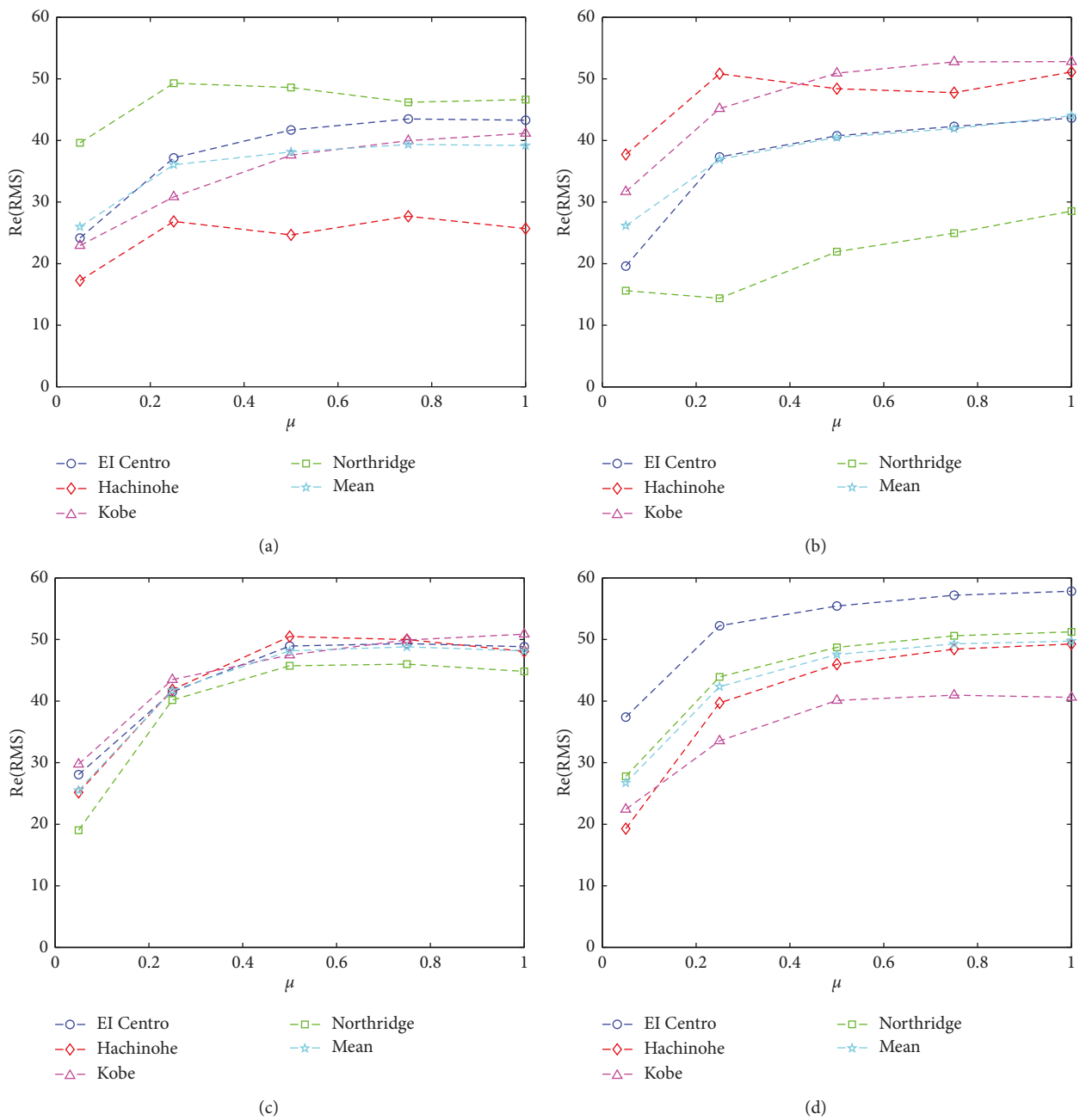

Figure 13: The damping effect of different mass ratios (TMD) on the mean square root of structural displacement response. (a) $T = 0.5$ s. (b) $T = 1.0$ s. (c) $T = 2.0$ s. (d) $T = 3.0$ s.

$$\mathrm{RMS}(x) = \mathrm{sqrt}\left(\frac{1}{N}\sum_{i=1}^{N} x_i^2\right), \tag{20}$$

where x_i is the structural displacement response corresponding to the i_{th} time and N is the total number of points collected.

Re(Peak) and Re(RMS) of the displacement response with different mass ratio TMDs are shown in Figures 12 and 13. The following conclusions can be obtained:

(1) TMD can effectively control the displacement response of the structure, and the large mass ratio (>0.25) TMD is more effective than the conventional small mass ratio (<0.05) TMD. But it can also be found that when the mass ratio of the TMD is greater than 0.5, the gain effect will diminish with increasing mass ratio;

(2) The TMD with the same mass ratio shows certain discreteness for the structures with different natural vibration periods and different seismic waves. For example, as shown in Figure 12(b), when the structure's period is 1.0 s, the damping rate of four seismic waves is distinct. When the mass ratio is 0.5, the minimum damping rate is 10.47% and the

Table 3: Maximum peak value of relative displacement between a TMD with optimal parameters and the main structure (cm).

T (s)	μ	El Centro	Hachinohe	Northridge	Kobe	Mean
0.5	0.05	4.36	2.96	3.81	3.12	3.56
	0.10	2.68	2.14	2.98	2.2	2.5
	0.50	2.14	2.54	3.35	1.91	2.49
	0.75	1.83	2.6	2.75	2.79	2.49
	1.00	2.24	2.74	2.24	3.37	2.65
1.0	0.05	8.18	8.83	10.39	6.98	8.59
	0.10	3.53	4.83	5.12	5.98	4.87
	0.50	3.41	5.35	3.76	5.88	4.6
	0.75	3.91	5.9	3.55	5.46	4.7
	1.00	3.56	4.94	3.58	5.02	4.28
2.0	0.05	14.77	20.9	8.66	18.34	15.67
	0.10	7.94	11.97	5.54	10.42	8.97
	0.50	5.3	8.63	4.17	8.58	6.67
	0.75	3.94	7.95	3.45	7.05	5.6
	1.00	3.89	8.46	3.32	6.29	5.49
3.0	0.05	15.09	35.29	6.66	19.93	19.25
	0.10	6.82	13	3.78	8.89	8.12
	0.50	4.91	11.28	3.29	6.54	6.51
	0.75	4.63	10.37	2.93	5.53	5.86
	1.00	5.09	11.25	2.62	5.36	6.08

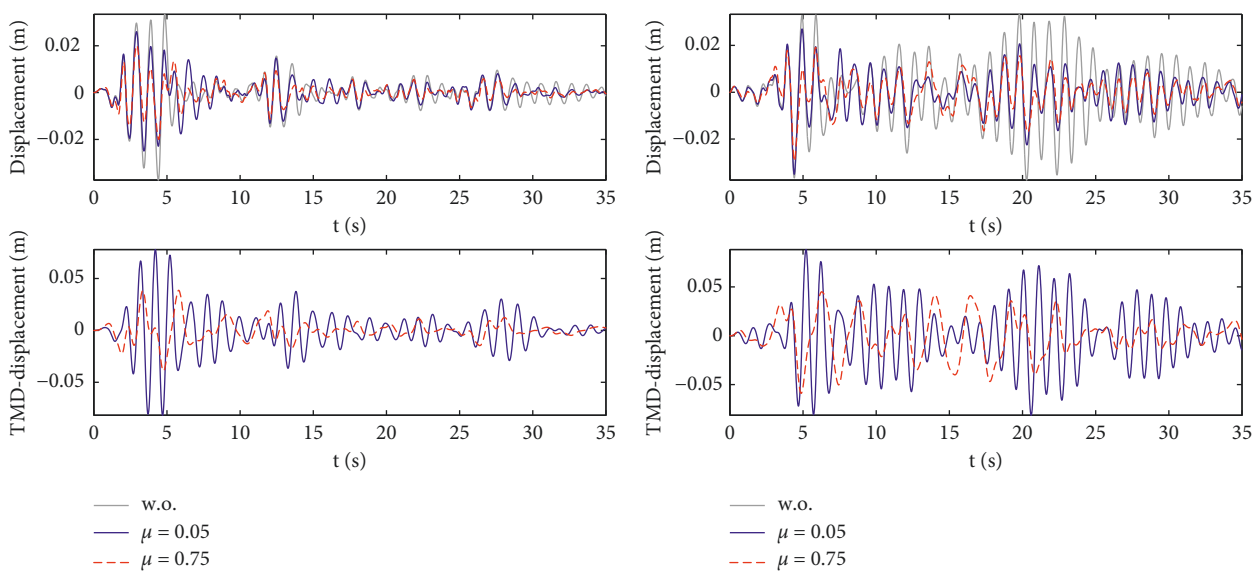

(a) (b)

Figure 14: Continued.

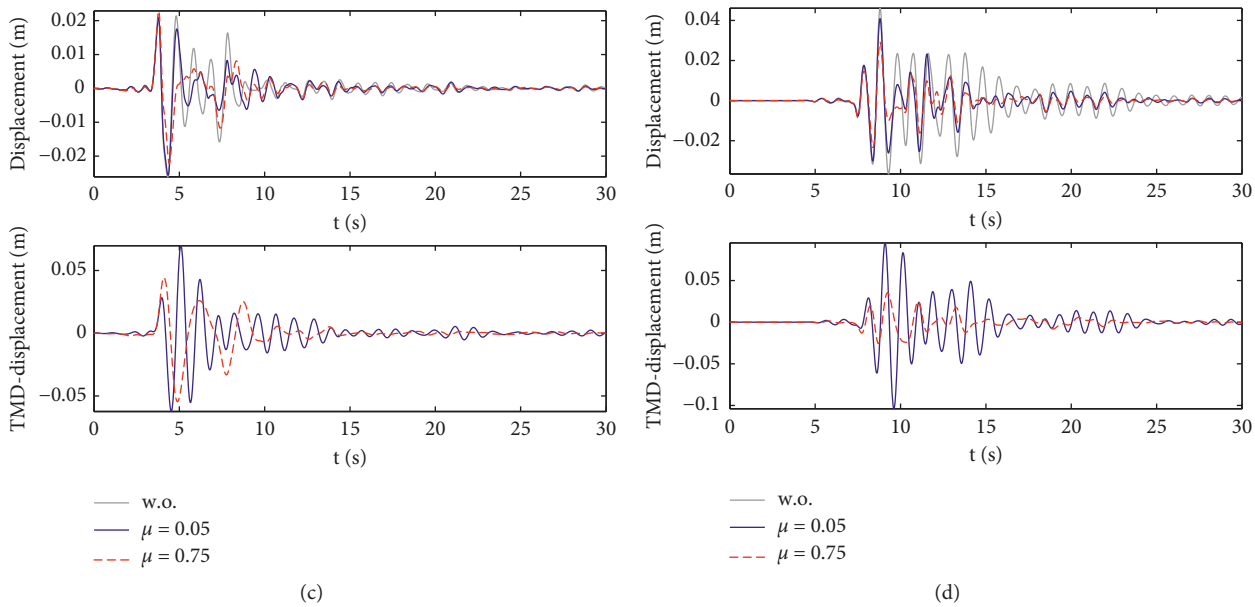

Figure 14: The damping effect of different mass ratio TMDs on the displacement-time history of the main structure ($T = 1.0$ s) and the relative displacement-time history between the TMD and the structure (w.o. denotes the displacement of a structure without a TMD). (a) El Centro. (b) Hachinohe. (c) Northridge. (d) Kobe.

maximum is 46.22%, which is usually mainly due to the difference in the frequency relationship between the structure and the seismic waves.

Table 3 shows the statistical results of the relative displacement between the TMD and main structure under different time history analysis conditions. It can be seen that the relative displacement between the TMD and the main structure is inversely proportional to the mass ratio of the TMD; that is, when a large mass ratio TMD is used, the displacement response of the structure is effectively controlled and the displacement stroke of the TMD is clearly reduced, which reduces the requirements for the elastic components and the damping components used to construct the TMD.

The displacement time histories of the structures with periods of 1.0 and 2.0 s and the relative displacement time histories between the TMD and the structures are shown in Figures 14 and 15, respectively. The schemes of mass ratios of 0.05 and 0.75 are compared. It can be clearly seen that the effect of a TMD in controlling the structural response and the TMD displacement stroke is more obvious for the TMD with a mass ratio of 0.75 than for the one with a mass ratio of 0.05.

In summary, the large mass ratio TMD has a more significant effect in seismic control of the main structure than the small mass ratio TMD.

6. Conclusions

In order to control the dynamic response and improve the aseismic performance of a structure, a large mass ratio TMD damping system is formed by using the equipment in the building structure or relying on new structural forms. The existing optimal parameter fitting formula is not applicable to large mass ratio TMDs, so it is revised by numerical optimisation and curve fitting, and the dynamic time history analysis method is used to study the effect of vibration damping control of large mass ratio TMDs. The following conclusions are obtained.

Compared with the traditional small mass ratio (<0.05) TMD, the large mass ratio (>0.5) TMD has obvious advantages in controlling the displacement response of the main structure. The control effect is about 1.5~3.25 times higher, the damping effect of the structural displacement peak can reach about 30%, and the damping ratio of the root mean square displacement can reach about 43.6%. At the same time, the relative stroke between the TMD and the main structure can be reduced with up to 30%~65%, which is highly beneficial to the practical engineering design of TMD structures.

When the mass ratio of a TMD is relatively large (>0.2), the results calculated by the existing fitting formula differ significantly from the actual optimal value, and the calculated values of the revised formula proposed in this paper are shown to be in good agreement with the actual optimal value. In general, the revised formula can be applied to both traditional small mass ratio and large mass ratio (≤1) TMDs. When the mass ratio is greater than 1, the optimal parameters of TMD can also be obtained by the method presented in this paper.

When the mass ratio is greater than 0.2, the optimal parameters of the stationary white noise random load and that of the filtered white noise random load are more similar, but the difference between the two is gradually increased with the increase of the TMD mass ratio. For the optimal parameters of large mass ratio TMDs (>0.2), the error is less than 0.05 when the ratio of the predominant frequency of the

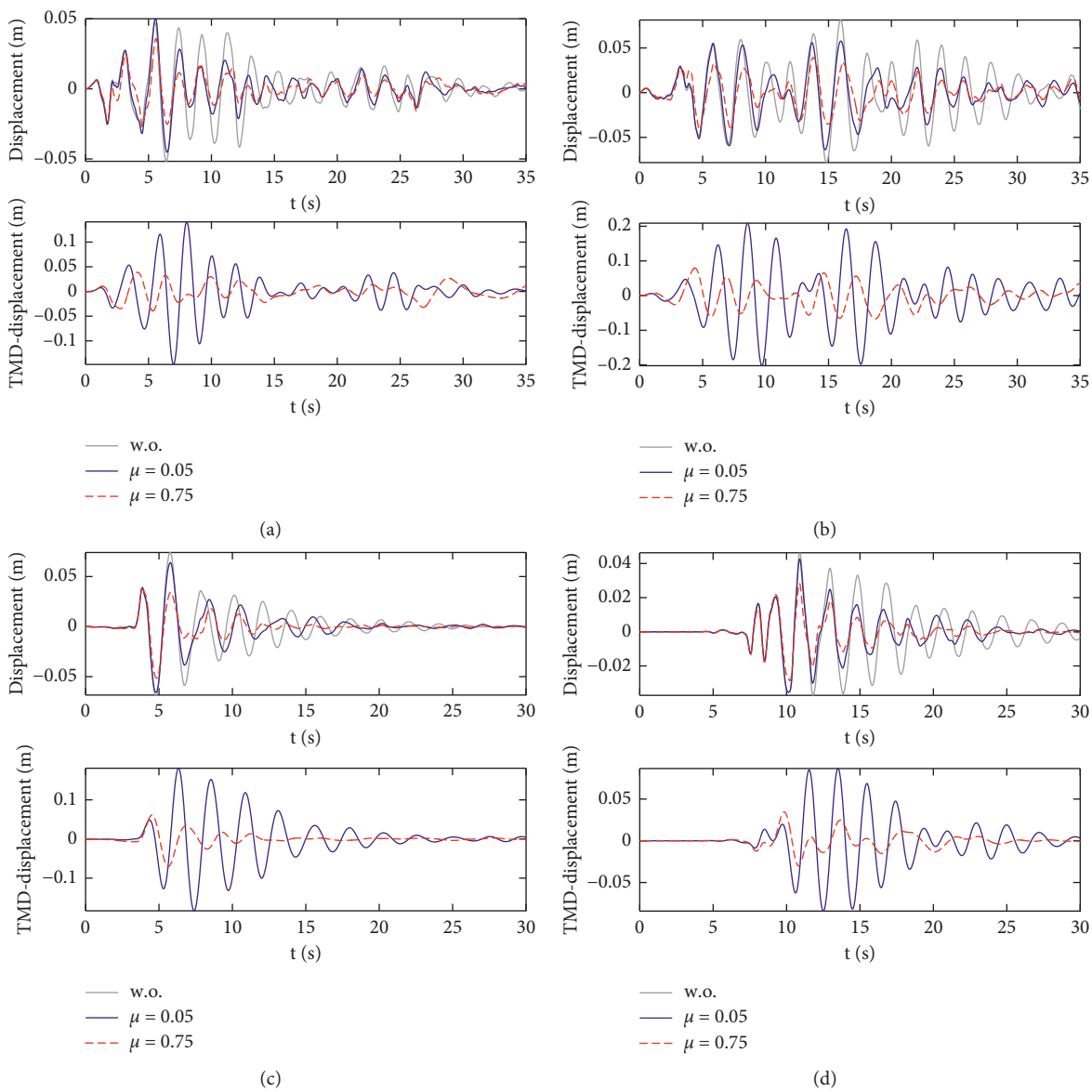

Figure 15: The damping effect of different mass ratio TMDs on the displacement-time history of the main structure ($T = 2.0$ s) and the relative displacement-time history between the TMD and the structure (w.o. denotes the displacement of a structure without a TMD). (a) El Centro. (b) Hachinohe. (c) Northridge. (d) Kobe.

base soil and the vibration frequency of the structure is greater than 4, and the optimal parameters of the TMD can be calculated by the fitting formula proposed in this paper. Under other conditions, it is suggested to use an optimisation method to determine the optimal value of TMD parameters.

At present, the actual engineering projects with large mass ratio TMD damping systems are less prominent, but their aseismic advantages will bring a broad range of benefits for research and practice.

Data Availability

The data used to support the findings of this study are available from the corresponding author upon request.

Conflicts of Interest

The authors declare that there are no conflicts of interest regarding the publication of this article.

Acknowledgments

This research was supported by Grant no. 51478023 from the National Natural Science Foundation of China.

References

[1] M. Gutierrez Soto and H. Adeli, "Tuned mass dampers," *Archives of Computational Methods in Engineering*, vol. 20, no. 4, pp. 419–431, 2013.

[2] S. Elias and V. Matsagar, "Research developments in vibration control of structures using passive tuned mass dampers," *Annual Reviews in Control*, vol. 44, pp. 129–156, 2017.

[3] D. Wang, T. K. T. Tse, Y. Zhou, and Q. Li, "Structural performance and cost analysis of wind-induced vibration control schemes for a real super-tall building," *Structure and Infrastructure Engineering*, vol. 11, no. 8, pp. 990–1011, 2014.

[4] N. Longarini and M. Zucca, "A chimney's seismic assessment by a tuned mass damper," *Engineering Structures*, vol. 79, pp. 290–296, 2014.

[5] L. Tian and Y. Zeng, "Parametric study of tuned mass dampers for long span transmission tower-line system under wind loads," *Shock and Vibration*, vol. 2016, Article ID 4965056, 11 pages, 2016.

[6] N. Hoang, Y. Fujino, and P. Warnitchai, "Optimal tuned mass damper for seismic applications and practical design formulas," *Engineering Structures*, vol. 30, no. 3, pp. 707–715, 2008.

[7] J. P. Den Hartog, *Mechanical vibrations*, McGraw-Hill, New York, NY, USA, 1956.

[8] G. B. Warburton, "Optimum absorber parameters for various combinations of response and excitation parameters," *Earthquake Engineering & Structural Dynamics*, vol. 10, no. 3, pp. 381–401, 1982.

[9] H.-C. Tsai and G.-C. Lin, "Explicit formulae for optimum absorber parameters for force-excited and viscously damped systems," *Journal of Sound and Vibration*, vol. 176, no. 5, pp. 585–596, 1994.

[10] H.-C. Tsai and G.-C. Lin, "Optimum tuned-mass dampers for minimizing steady-state response of support-excited and damped systems," *Earthquake Engineering & Structural Dynamics*, vol. 22, no. 11, pp. 957–973, 1993.

[11] S. V. Bakre and R. S. Jangid, "Optimum parameters of tuned mass damper for damped main system," *Structural Control and Health Monitoring*, vol. 14, no. 3, pp. 448–470, 2007.

[12] C. C. Lin, C. M. Hu, J. F. Wang, and R. Y. Hu, "Vibration control effectiveness of passive tuned mass dampers," *Journal of the Chinese Institute of Engineers*, vol. 17, pp. 367–376, 1994.

[13] A. Y. T. Leung and H. Zhang, "Particle swarm optimization of tuned mass dampers," *Engineering Structures*, vol. 31, no. 3, pp. 715–728, 2009.

[14] M. Q. Feng and A. Mita, "Vibration control of tall buildings using mega SubConfiguration," *Journal of Engineering Mechanics*, vol. 121, no. 10, pp. 1082–1088, 1995.

[15] X. X. Li, P. Tan, X. J. Li, and A. W. Liu, "Mechanism analysis and parameter optimisation of mega-sub-isolation system," *Shock and Vibration*, vol. 2016, p. 12, 2016.

[16] A. Reggio and M. D. Angelis, "Optimal energy-based seismic design of non-conventional tuned mass damper (TMD) implemented via inter-story isolation," *Earthquake Engineering & Structural Dynamics*, vol. 44, no. 10, pp. 1623–1642, 2015.

[17] S. J. Wang, B. H. Lee, W. C. Chuang, and K. C. Chang, "Optimal dynamic characteristic control approach for building mass damper design," *Earthquake Engineering & Structural Dynamics*, vol. 47, no. 3, 2017.

[18] H. Anajafi and R. A. Medina, "Partial mass isolation system for seismic vibration control of buildings," *Structural Control & Health Monitoring*, vol. 25, no. 2, article e2088, 2017.

[19] K. Yuan, M. S. He, and Y. M. Li, "Shaking table tests for energy-dissipation steel frame structures with infilled wall MTMD," *Journal of Vibration and Shock*, vol. 33, no. 11, pp. 200–207, 2014.

[20] R. Ding, M. X. Tao, M. Zhou, and J. G. Nie, "Seismic behavior of RC structures with absence of floor slab constraints and large mass turbine as a non-conventional TMD: a case study," *Bulletin of Earthquake Engineering*, vol. 13, no. 11, pp. 3401–3422, 2015.

[21] L. Y. Peng, Y. J. Kang, Z. R. Lai, and Y. K. Deng, "Optimisation and damping performance of a coal-fired power plant building equipped with multiple coal bucket dampers," *Advances in Civil Engineering*, vol. 2018, p. 19, 2018.

[22] Z. Shu, S. Li, J. Zhang, and M. He, "Optimum seismic design of a power plant building with pendulum tuned mass damper system by its heavy suspended buckets," *Engineering Structures*, vol. 136, pp. 114–132, 2017.

[23] K. Dai, B. Li, J. Wang et al., "Optimal probability-based partial mass isolation of elevated coal scuttle in thermal power plant building," *Structural Design of Tall and Special Buildings*, vol. 27, no. 11, article e1477, 2018.

[24] M. De Angelis, S. Perno, and A. Reggio, "Dynamic response and optimal design of structures with large mass ratio TMD," *Earthquake Engineering & Structural Dynamics*, vol. 41, no. 1, pp. 41–60, 2015.

[25] K. Kanai, "Semi-empirical formula for the seismic characteristics of the ground," *Bulletin of the Earthquake Research Institute, The University of Tokyo*, vol. 35, pp. 309–325, 1957.

[26] *Code for seismic design of buildings*, GB50011-2010, Beijing, China, 2010.

[27] B. F. Spencer, R. E. Christenson, and S. J. Dyke, "Next generation benchmark control problem for seismically excited buildings," in *Proceedings of the 2nd World Conference on Structural Control*, pp. 1351–1360, Kyoto, Japan, June 1998.